International Journal on Recent and Innovation Trends in Computing and Communication
ISSN: 2321-8169 Volume: 11 Issue: 9
***Article Received:** 25 July 2023 **Revised:** 12 September 2023 **Accepted:** 30 September 2023*

Optimal Prediction and Disease Severity Classification of Proteomic Survival in Pre and Post-Covid-19 Using Hybrid Machine Learning Approach

Jagannath Jijaba Kadam[1*], Siddhanath Abasaheb Howal[2], Mahadeo Ramchandra Jadhav[3], Ganpati Martand Kharmate[4], Vikram Uttam Pandit[5]

[1*]Professor, Chemistry Department, Bharati Vidyapeeth college of Engineering, Navi Mumbai, India, Email: jjkadam702@gmail.com

[2]Assistant Professor, Gharada Institute of Technology, A/P Lavel, khed, Ratnagiri, Maharashtra, India, Email: siddhu.howal@gmail.com

[3]Assistant Professor, Chemistry Department, Bharati Vidyapeeth college of Engineering, Navi Mumbai, India, Email: mahadeojadhav2013@gmail.com

[4]Assistant Professor, Physics Department, Bharati Vidyapeeth college of Engineering, Navi Mumbai, India, Email: ganpati.kharmate@bvcoenm.edu.in

[5]Assistant Professor, Haribhai V. Desai College, Pune-411002, Maharashtra, India, Email:vikramupandit@gmail.com

Abstract: Uncertainty surrounds the underlying mechanisms of the severe COVID-19 disease of 2019. The capability to detect COVID-19 through artificial intelligence techniques, particularly deep learning, will help to do so in the early stages, which will increase the likelihood that patients around the world will recover rapidly. The load on the healthcare system globally will be relieved as a result. Several thousand plasmas and serum proteins from COVID-19 patients and symptomatic controls are longitudinally analysed in this study to identify non-immune and immune proteins associated with COVID-19. The development of predictive models thus involves taking into account the topological variations across networks from different scenarios (survivors vs. non-survivors). As a result, the study's test subjects, who weren't included in the machine learning (ML) training, had high prediction accuracy. This study successfully predicted the existence of critically ill (CI) patients both before and after COVID-19 by using an MLM built on a synonymic network that incorporates measurements of several proteins. A rise in some acute phase and inflammatory proteins (IP) with time (e.g. ITIH3, SAA1; CRP, SAA2, LBP, SERPINA1, and LRG1) is related to the danger of death after COVID-19, while an upsurge of kallikrein (KLKB1), kallistatin (SERPINA4), thrombin (F2), Apo lipoprotein C3 (APOC3), GPLD1, and the protease inhibitor A2M, is associated with survival. The same clinical symptoms, such as dry cough, fever, squatness of breath, and others, are linked to both severe and critical patients. The lesion outlines are then retrieved from the COVID-19-contaminated regions after the entropy texture features have been extracted using a Gray-level co-occurrence Matrix (GLCM) to confirm the infected regions (IR). Further, the study implemented a variety of features using CT images with a CNN-based Inception V3 model for selection algorithms to filter significant features. Finally, construct a model of transfer learning (TL) using the VGGNet16 model which could capture and further classify the disease severity. Based on Matlab software, the suggested work is assessed. With a compassion of 96.7% and specificity of 98.2%, the results demonstrate that VGGNet16 is the most suitable TL model to identify COVID-19, nonetheless, it also exceeds the most advanced methods at the moment. The clotting system and accompaniment cataract are home to the bulk of proteins in the forecast model with high significance. This work shows that plasma proteomics (PP) can result in prognostic predictions that vastly outperform the present prognostic markers in critical care, respectively.

Keywords: COVID-19, Synolytic Network, VGGNet16 Model, Gray-Level Co-Occurrence Matrix, Disease Severity, Convolution Neural Network, and Inception V3 Model.

I. INTRODUCTION

The SARS-CoV-2 outbreak that gave rise to the COVID-19 sickness in December 2019 swiftly snowballed into a devastating global healthcare disaster. Human-to-human transmission of Covid-19 is made easier by respiratory droplets produced by coughing and sneezing. Comprehensive blood amount, C-reactive protein (CRP), clotting tests, D-dimer, ferritin, lactic dehydrogenase (LDH) and procalcitonin are the laboratory tests applied to detect the severity of disease, myocardial damage, thromboembolic complications, and/or worse prognosis [1]. For COVID-19, a quantity of replicas has been shaped to determine the level of disease severity and the prediction of clinical outcomes. These models are based on laboratory testing, imaging, and omics technology. Recognizing new biomarkers related to disease severity is essential to help identify patients with the high possibility of developing a critical illness to target the allocation of resources, the intensification of care, and the addition of experimental clinical trials to those who are in most need [2]. The potential prognosticators of COVID-19 severity or impermanence have already been identified as D-dimer, lactate dehydrogenase, and CRP[3]. With their aptitude to identify several proteins in a single analysis, proteomics technologies have started to extend

International Journal on Recent and Innovation Trends in Computing and Communication
ISSN: 2321-8169 Volume: 11 Issue: 9
***Article Received:** 25 July 2023 **Revised:** 12 September 2023 **Accepted:** 30 September 2023*

these preliminary findings. Rapidly conducted research and development on a global basis has already produced analyses for detecting host immunoglobulins and SARS-CoV-2 RNA [4].

Protein-protein interactions, post-translational modifications, the temporal pattern of expression, and cellular and sub-cellular delivery are all factors that are taken into consideration during proteome analysis, which also seeks to uncover the numerous ways that proteins manifest themselves. Data generated by differential and functional proteomics contributes to a better comprehension of biological pathways and how they are related to cells and living things [5]. Mass spectrometry methods for protein identification and delineation have overcome the limitations of earlier proteome technologies, such as 2D gels, which require a significant quantity of pure proteins for analysis [6]. Since proteomic techniques can provide information on the various protein expressions and their post-translational modifications (PTMs), they are suitable for evaluating COVID-19 for they can identify the factors that drive abnormal cellular mechanisms and specific illness states [7].

PP provides insightful information regarding the course of the disease and potential treatments. Most research now focuses on the diagnosis of COVID-19 biomarkers based on untargeted shotgun proteomics generating relative quantitative data of poor precision and expensive cost-of-the-art apparatus which is delicate to manage [8]. In the plasma of COVID-19 patients, recent proteomic investigations identified molecular alterations that were consistent with severe dysregulation of several inflammatory responses (IR) characteristics, in addition to an overall metabolic conquest. Twelve serum protein structures and a perfect of seven common clinical tests were identified using PP and lab clinical tests as first risk prognosticators of COVID-19 severity and patient survival in SARS-CoV-2 affected patients [9]. Time-based patient molecular phenotypes depict an initial stage of the full IR, which is then gradually intensified and is trailed by a protein structure that represents metabolic reconstitution, tissue healing, and immunomodulation [10]. Developed a thorough molecular picture of how the patient's molecular phenotype varies depending on the age, severity, and stage of the disease by linking the collection of diagnostic constraints with the proteomes in a patient time-resolved manner [11]. AI is utilized to analyze, display, and understand intricate medical and health data. The capability of computer programs to guess assumptions based mainly on input data is known as artificial intelligence [12]. The most important objective of health-associated AI applications is to discover how clinical procedures affect patient outcomes [13]. The ML-based models possess a huge perspective to forecast the existence balances of COVID-19-affected patients in the initial stages of the virus infection and at the period of treatment [14]. ML methods have been secondhand to examine different biological datasets, including proteomics, NGS, and metabolomics data, to predict the biomarkers for the classification of samples and genes linked to a particular illness state [15]. Although imaging methods are utilized to diagnose COVID-19, to the knowledge no research has employed imaging to distinguish between critical cases and severe cases. PP combined with ML-based models are utilized in this study to help solve the aforementioned issue [16]. Analysing reactions to SARS-CoV-2 is the research's driving force. Identify protein signatures linked to COVID-19 infection, severity, and death using two unbiased PP techniques in a sizable population of critically sick patients awarded to a sizable built-up emergency department (ED). The residue of the work is divided into the following sections: section 2, which illustrates the study's literature review; section 3, which illustrates the work's problem definition and motivation; and section 4, which illustrates the suggested research technique. Section 5 describes the experimentation and results in detail, while Section 6 discusses the research's conclusions.

II. Literature Survey

Wenyu Chen *et al*. [17] proposed a collective estimate model for severe COVID-19 pneumonia that depends on clinical aspects combined with clinical aspects, pulmonary lesion volume, and radionics structures of patients and has a significant differential ability for forecasting the sequence of the disease in COVID-19 patients. This might help in the early detection and treatment of severe COVID-19 symptoms. With an 86% sensitivity and 85% specificity, CT radionics features removal and examination founded on a deep neural network (DNN) may identify COVID-19 patients.

According to H Yan *et al*. [18], COVID-19 patients with great serum LDH values exhibited differentially expressed blood coagulation responses and immune, including acute IR, complement cascades, platelet degranulation, and numerous different metabolic responses, counting lipid metabolism, protein ubiquitination, and pyruvate fermentation. Patients with raised LDH values were focused on their activation of hypoxic reactions. Serum LDH levels correlate with COVID-19 severity, and high serum LDH may result from tissue damage brought on by inflammation and hypoxia.

PA study group [19] proposed that the evaluation of 321 blood protein expression groups in 50 CI COVID-19 patients getting aggressive mechanical air conditioning exposed 14 proteins that presented trajectories different among non-survivors and survivors. Proteomic measurements were acquired at the supreme treatment level (TL) which was weeks earlier than the consequence attained the accurate classification of survivors. PP can give enlargement to prognostic predictors significantly outperforming present predictive markers in concentrated care.

Evaluation of 50 CI patients' 321 serum protein expression categories was suggested by the PA study group [19]. 14 proteins with distinct trajectory differences among non-survivors and survivors were found in COVID-19 patients receiving aggressive mechanical breathing. Proteomic measurements were taken at the highest TL, weeks before the correct classification of survivors was achieved. PP can considerably improve prognostic predictions in critical care, exceeding current predictive markers.

According to Zili Zhang *et al*. [21], 445 Differentially Expressed Proteins (DEPs) were discovered in distinct comparison groups out of the total acknowledged and counted proteins. 11 proteins were only found in COVID-19 individuals, in contrast to COPD and asthma. Functional analyses revealed that most of them were related to platelet activation, coagulation cascades, iron metabolism, and anaemia-related pathways Seven of the 84 proteins found in the main investigation, including von Willebrand issue type A and Ephrin type-A

International Journal on Recent and Innovation Trends in Computing and Communication
ISSN: 2321-8169 Volume: 11 Issue: 9
***Article Received:** 25 July 2023 **Revised:** 12 September 2023 **Accepted:** 30 September 2023*

receptor 4, were suggested by Steffen *et al* [22] to be significantly linked to hospitalised respiratory infections.

According to DRS Junior *et al*. [23], hospitalised patients' levels of apolipoprotein F (APOF), serum amyloid A 1 and 2 (SAA1 and SAA2, respectively), inter-alpha-trypsin inhibitor heavy chain H4 (ITIH4), pulmonary surfactant-associated protein B (SFTPB), and HDL-C increased by additional than 50% when compared with patients who had only mild symptoms. This improvement occurred regardless of sex. According to Foo *et al*. [24], COVID-19-affected pregnant women mounted substantial IR together with strong activation of the IFNL1/IFNLR1 axis. They emphasise the significance of prolonged clinical monitoring of mother-infant dyads following COVID-19+ pregnancies.

In contrast to bagging (91.84%) and voting (93.88%), Seyma Yazer *et al*.'s [25] research showed that adaboost (96.00%) had a better accuracy rate. The maximum accuracy (97.92%) was achieved with the Stacking collaborative learning method. The most important proteins connected to the severity of the disease were GSN, SERPINA1, SERPING1, and SERPINA3. In comparison to the alternative approaches, the proposed ensemble learning model (Stacking) demonstrated the best assessment of illness severity based on proteins. According to Poulos *et al*. [26], DIA-MS has been operated to uncover protein biomarkers that are involved in COVID-19 risk classification. These protein biomarkers can be combined with medication therapy recommendations based on the disease's progression [27]. Pharmacoproteomics presents a novel approach to add value to drug discovery, development, and repurposing processes in addition to polypharmacology, drug metabolism investigations, and drug testing procedures [28]. After reviewing the available studies, the primary objective of this project is to longitudinally analyse thousands of plasma and serum proteins from COVID-19 patients and asymptomatic controls to classify resistant and non-immune proteins associated with the disease [29].

III. Research Problem Definition And Motivation

Globally, the COVID-19 disease of 2019 has resulted in over 1 million fatalities. The disease can cause serious illness, organ malfunction, and death, or it might cause only an asymptomatic carrier status. Most CI COVID-19 patients are being accommodated by healthcare systems in large numbers across the globe [30]. Additionally, the epidemic makes it urgently essential to accelerate clinical trials observing potential novel treatments [31]. While multiple biomarkers can differentiate between individuals with varying illness severity and predict the future course of disease for those patients, prognosis is still challenging for patient groups with similar disease severity, such as those needing intensive care [32]. To the information, no studies have utilized medical imaging to distinguish between critical cases and severe patients [33].

Although multi-omic techniques are starting to circumvent these restrictions, much research addressing the immune response to severe acute respiratory syndrome-coronavirus-2 (SARS-CoV-2) is constrained by small sample sizes or analysis-specific subsets of immune mediators [34]. Discover protein signatures linked to COVID-19 infection, severity, and death by examining responses to SARS-CoV-2 using two unbiased PP techniques in a sizable cohort of critically unwell patients given to a sizable urban emergency department (ED) [35]. Studies map them to specific cell types in the setting of pertinent clinical characteristics [36–38] to get insights into the underlying illness mechanisms. PP can be the cornerstone of a new group of predictors since it bears the promise of merging an individual's genetic background with life history, and physiological, dietary, and demographic factors [39-40].

IV. Proposed Research Methodology

Hospital admissions due to the COVID-19 disease 2019 have recently surged dramatically, placing a significant strain on healthcare systems all over the world and raising the need for accurate diagnostics that can forecast the severity and fatality of the disease [41-45]. This study precisely assessed the amounts of hundreds of proteins and metabolites in plasma from hospitalised COVID-19 patients using multiplexed targeted mass spectrometry assays using a reliable triple quadrupole MS system that is available in many clinical laboratories [46-50]. A surprisingly substantial difference among both living people and dead people along with a noticeable differentiation between COVID-19 patients and controls were noted by the researchers [51-53; 54-56]. Block representation of the suggested model is shown in figure 1.

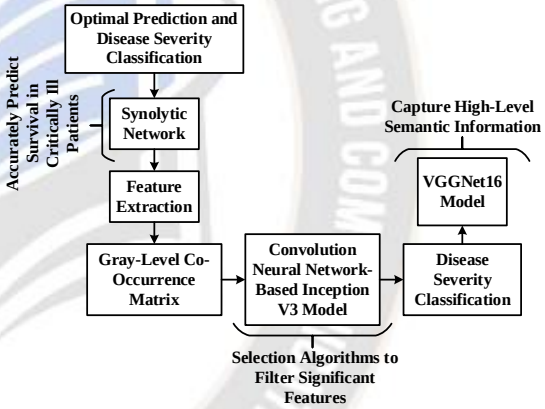

Figure 1. Block Diagram of the Proposed Work

A. Feature Segmentation and Extraction

Identifying illness severity requires the extraction of high-throughput data. The team then separated the lung area for texturing and twisted a DL model by manually extracting features [57-58]. To classify severe and critical cases, second, select the best hand-crafted feature subset from the features that were initially chosen. The COVID-19 IRs are first confirmed by extracting the contrast, coarseness, roughness, and entropy texture features using a GLCM, after which the lesion contours are retrieved from the infected areas.

1. Texture Features

A traditional technique for texture analysis involves combining the elements that are taken from the grey-level co-occurrence matrix (GLCM). Denoised photos serve as its input, while segmented images at first are its output. The process is complete when the segmentation contour matches the prior contour. Lesion outlines are then retrieved from the COVID-19-

International Journal on Recent and Innovation Trends in Computing and Communication
ISSN: 2321-8169 Volume: 11 Issue: 9
***Article Received:** 25 July 2023 **Revised:** 12 September 2023 **Accepted:** 30 September 2023*

IRs after the COVID-19 IRs have been confirmed using the GLCM.

Gray-Level Co-Occurrence Matrix

The GLCM, which represents texture features, is retrieved. In an image space $M \times N$ (ROI) spanning from grey level 0 to $Q-1(Q=256)$, the 'e GLCM builds the mutual occurrence of various grey levels i, j between a pair of pixels unglued by a specific distance d and orientated in a specific direction. The GLCM element can thus be described as follows:

$$q(i,j) = [(k,l),(m,n)](m)-k = x*d, n-l = y* d, I(k,l) = i, I(m,n) = j \quad (1)$$

Where, (k,l), (m,n) represent the pixels in the ROI, $I(\cdot)$ denotes the pixel's level of grey, and n represents the amount of pixels that satisfy the criterion. The standards of the parameters x, y at various for direction $\theta = 0°, 45°, 90°$, and 135°. Each element in the GLCM in this article should be a probability value that has undergone a normalisation process, and the GLCM itself requirement be symmetrical for the texture computation. According to its definition, the element of the normalised grey-level co-occurrence matrix (NGLCM) is,

$$p(i,j) = \frac{q(i,j)}{\sum_{i=0}^{Q-1}\sum_{j=0}^{Q-1} q(i,j)} \quad (2)$$

A colour image is converted into an image of grayscale as input. A grayscale or grey-scale image is one in which the worth of respectively pixel is a single example indicating only a quantity of light, that is, it conveys only intensity information, in photography, computing, and calorimetry. This study will custom GLCM, a statistical technique for analysing texture that takes into account the spatial association of pixels, to analyse the textural characteristics of the surface unevenness of mangos teens.

This technique has proven to be a general way to extract texture features from images since it determines the frequency of pixel pairs in the image that have the same grey level. The reason that GLCM is referred to as a second-order statistic is that it gathers data on pairs of pixels rather than a single one, is based on statistical analyses of the supply of pixel intensity and expresses the probabilities $P(i,j|d,\theta)$ of two pixels appearing together with intensities (i,j) and relative polar coordinates (d,θ). It can also be described as the total amount of times that a pixel in the contribution image that has an intensity grey-level value of (i) happened in a connection to a pixel that has a value of (j), multiplied by the number of times. As a result, the following variables need to be supplied before the GLCM feature is computed.

1. The pixel of interest (reference) is applied to determine the spatial connection (angle),

and the neighbouring pixels can only be at an angle of 0°, 45°, 90°, or 135°.

2. An integer number, d can have a value of $(1,2,3,\ldots n)$, and it represents the displacement vector $d=(dx,dy)$ between the interest pixel and its neighbouring pixel over the image.

3. The quantity of grey levels (G), where G is typically either 4, 8, 16, or 32. The quantity of (G) controls the scope of the GLCM.

A 2D (square) dependency GLCM matrix is the result. The GLCM is normalised by the total of the elements to produce a probability matrix. Depending on the different values of (θ and d) that are exploited to extract it, the study can obtain a variety of GLCM matrices.

Notation

$p(i,j)$A normalised gray-tone spatial dependency matrix's $p(i,j)$th entry is equal to $= P(i,j)/R$.

R is the normalizing constant. $R = \sum_{i,j=1}^{N_g} P(i,j)$

The matrix of marginal probabilities' ith element is$p_x(i)$.

N_g is the amount of separate grey stages in the image quantized.

GLCM Properties

The suggested CBIR system in this study usages the GLCM attributes listed below as texture features:

Contrast: Provides a measurement of the overall intensity contrast among a pixel and its neighbour:

$$f_2 = \sum_{n=0}^{N_g-1} n^2 \left\{\sum_{i=1}^{N_g}\sum_{j=1}^{N_g} p(i,j)\right\} \quad (3)$$

Correlation: Gives a measurement of how correlated each pixel is with each of its neighbours across the entire image:

$$f_3 = \frac{\sum_{i,j}(ij)p(i,j)-\mu_x\mu_y}{\sigma_x\sigma_y} \quad (4)$$

Where, μ_x, μ_y, σ_x and σ_y are the standard nonconformities and means of $p_x$and p_y

Variance

$$f_4 = \sum_{i,j}(i-\mu)^2 p(i,j) \quad (5)$$

Energy: Returns the GLCM's squared element sum:

$$\sum_i \sum_j p^2(i,j)$$

Homogeneity: Returns a value indicating how closely the circulation of GLCM elements resembles the diagonal of the GLCM:

$$\sum_i \sum_j \frac{p(i,j)}{1+|i-j|} \quad (6)$$

The GLCM mean μ (which is a measure of the brightness of all pixels in the connections that are invested to the GLCM) and the variation of the magnitudes of all regarded pixels in the interactions that contributed to the GLCM are each represented by Pi,j, which stands for the components of the normalised symmetrical GLCM.

2. Convolution Neural Network-Based Inception V3

The foundational layer of CNN is a convolutional layer (CL). It is in charge of figuring out the pattern's characteristics. The participation image is run through a filter in this layer. The feature map is made up of the values obtained during filtering. To extract the pattern's low- and high-level features, this layer applies certain kernels that slide across the pattern.

The CL's output can be expressed as follows:

$$x_j^l = f\left(\sum_{a=1}^{N} w_j^{l-1} * y_a^{l-1} + b_j^l\right) \quad (7)$$

Where x_j^l is the jth feature map in layer l, w_j^{l-1}denotes the jth kernels in layer $l-1$, y_a^{l-1}denotes the ath feature map in layer $l-1$, b_j^l denotes the bias of the jth feature map in layer l, N is the number of total features in layer $l-1$, and $(*)$ denotes the vector convolution process.

International Journal on Recent and Innovation Trends in Computing and Communication
ISSN: 2321-8169 Volume: 11 Issue: 9
***Article Received:** 25 July 2023 **Revised:** 12 September 2023 **Accepted:** 30 September 2023*

Pooling Layer

The pooling layer (PL) comes next after the CL. By using the appropriate mathematical computation, the PL is often applied to the developed feature maps to reduce the amount of feature maps and network parameters. Employed global average pooling and maximum pooling in this investigation. Reduced output neurons are the outcome of the max-pooling method, which customs the matrix size set in each feature map to select only the maximum value. Additionally, data is condensed to a single dimension using a worldwide average PL, which is only employed before the fully linked layer. Following the layer for the global average pooling, it is connected to the fully connected layer. The dropout layer is an extra intermediate layer that is employed.

Fully Connected Layer

The final and most significant layer of CNN is the fully connected layer. This layer performs the same tasks as a multilayer perceptron. On a fully connected layer, the rectified linear unit (ReLU) activation function (AF) is frequently utilised, nevertheless, the softmax AF is utilized to forecast output images in the last layer of the completely connected layer. These two AFs were calculated mathematically as follows:

$$ReLU(x) = \begin{cases} 0, if\ x < 0 \\ x, if\ x \geq 0 \end{cases} \quad (8)$$

$$Softmax\ (x_i) = \frac{e^{x_i}}{\sum_{y=1}^{m} e^{x_y}} \quad (9)$$

The input data x_i and the numeral of classes m are represented in this sentence, accordingly. Every AF in the layer before is fully coupled to each neuron in the layer below.

Pre-Trained Models

CNN models with millions of parameters demand equipment with great presentation and are exceedingly time-consuming to train from scratch. The parameters and weights of models developed using various datasets are exploited in the new model to address these issues. In addition to the transferred components, the newly added layers also aid in the learning process. Even in a slight quantity of datasets, it is claimed to be exceptionally successful. Additionally, studies may get results more swiftly and for less money by using this strategy.

The schematic illustration of a traditional CNN that includes pre-trained ResNet50, InceptionV3, ResNet152, ResNet101 and Beginning ResNetV2 representations for the forecast of healthy people, COVID-19 patients, and pneumonia caused by bacteria and viruses.

ResNet50

A better variant of CNN is the residual neural network (ResNet) model. To fix an issue, ResNet inserts shortcuts between layers. It avoids the distortion that develops as the network becomes more intricate and deeper. A 50-layer network called ResNet50 was developed using the database for ImageNet. For usage in image recognition competitions, ImageNet is a collection of images with more than 14 million photos organised into more than 20,000 categories.

InceptionV3

CNN model InceptionV3 belongs to this category. There are multiple convolutional and maximum pooling steps in it. It has a NN that is fully connected in the final stage. The ImageNet dataset is employed to train the network, much like it was for the ResNet50 model.

Inception-ResNetV2

Employing the Inception-ResNetV2 architecture and trained on the ImageNet dataset, the model comprises a deep convolutional network. A list of predicted probability classes is produced by the model and is given as input along with a 299 x 299 image.

ResNet101 and ResNet152

Due to loaded ResNet construction pieces, ResNet101 and ResNet152 have 101 and 152 layers, respectively. Import a network that has already been trained using data from the ImageNet folder and more than a million photos. Consequently, the network has selected detailed feature representations for a variety of images. The scope of the network's picture input is 224 by 224.

B. Prediction of Survival

To train the existence predictor, the first stretch argument observed at WHO score 7 was chosen for each patient. The 'future' data, encoded in the advanced time points, was prevented from being employed for forecaster exercise as a result. Restricted the amount of 57 proteins that are FDA-accepted biomarkers with MRM examines obtainable and that were enumerated with at least three separate peptides in this study to decrease the feature interplanetary applied as input for the MLM. The data were standardised, and values that were missing were imputed utilising minimal value imputation. The par enclitic network method was applied to the synonymic network. A circular SVM classifier is briefly trained during training for each pair of features (using the SVM () function from the "e1071" R package with avoidance values). The next stage is to form a network for each sample, where the edge weight (EW) is the SVM classifier's projected death probability and the vertices represent characteristics. The maximum, mean, and typical deviation of the EWs are determined, besides the proportion of nodes and edges with weights larger than 0.5 (i.e., a fatal outcome is projected). Then, using the glmnet () function of the "glmnet" R package with evasion defaults, a LASSO classification model (alpha = 0.01) is built on these 5 features.

A cross-validation method was employed to evaluate the presentation of the classifier (Charité cohort (CC)). For each example, a prediction was made by withholding it from the data*et al*ong with two other samples (selected at random with the restriction that out of three samples, one corresponds to a non-survivor and two to survivors), training the classifier on the other (independent) samples, and then producing predictions for the withheld sample. The forecasts for each sample were averaged after 50 random generations of such a leave-3-out partition. The partitioning technique made sure that any potential overfitting, no matter how big, would not have an impact on the assessment of the predictive routine. The

International Journal on Recent and Innovation Trends in Computing and Communication
ISSN: 2321-8169 Volume: 11 Issue: 9
***Article Received:** 25 July 2023 **Revised:** 12 September 2023 **Accepted:** 30 September 2023*

classifier was trained using all of the Charité samples, and it was then applied to the Innsbruck cohort to forecast the likelihood of fatal outcomes to evaluate its efficacy on an autonomous dataset (Innsbruck cohort). Additional materials include the source code. Proteins' "relevance" scores in the par enclitic model were determined by calculating Kleinberg's expert importance scores for each of the corresponding vertices in the "generalising network" In the networks belonging to non-survivors, EWs added than 0.5 were replaced with 1.0, and EWs less than 0.5 were replaced with 0.0. The resulting networks were then averaged.

1. Synolytic Network Approach

The underlying flaw in KDEPA is automatically fixed by the synoptic network method by normalising the detachment extent in terms of probability. Here, demonstrates the synolytic technique compared to other ML models and is occasionally even superior to them. One benefit is the aptitude to visually recognise key elements in the findings, which increases transparency for "black-box" ML algorithms. They provide the chance to investigate the generated networks using more advanced network analysis concepts, and they enable the examination of networks throughout time, inspiring future notions of par enclitic-longitudinal data investigation.

Here, validate that whereas an increase in thrombin (F2), kallistatin (SERPINA4), kallikrein (KLKB1), apolipoprotein C3 (APOC3), GPLD1, and the protease inhibitor A2M is associated with survival from COVID-19, a surge in exact provocative and severe stage proteins is associated to a higher chance of dying from COVID-19. Interestingly, in COVID-19, THE research team and others discovered that the expression of each of these proteins varied depending on the severity of the condition. Furthermore, there is a significant overlap with a COVID-19 panel of proteins that predict death. Thus, even though only a minor subset of proteins that are differentially focused contingent on the severity of the disease predict the outcome and that typical single-centre ICU studies are carried out on minor statistics of patients, this result indicates a high degree of congruence and reproducibility of plasma the proteome signatures across studies.

Acute-phase proteins including SERPINA1, CRP, ITIH3, SAA1, and SAA2 are also dysregulated in other IR like sepsis. In addition to the general pro-IR of these prognostic proteins, elevated LRG1 and LBP along with decreased A2M are signs of an ongoing immunological response. Since lipid metabolism is dysregulated in bacterial pneumonia and consequently associated with adverse outcomes, APOC3 and GPLD1 are involved in this process. Three known dysregulated mechanisms in COVID-19 are the complement cascade, fibrinolysis, and the blood thickening system, all of which require kallikrein. It facilitates the cleavage of kininogen to bradykinin and des-Arg9-bradykinin, a powerful vasoactive peptide that is inhibited by ACE2, the SARS-CoV-2 cell entry receptor. Inhibition of the kallikrein-kinin system has been planned as a treatment for COVID-19 for it has been hypothesised that the lack of ACE2 in COVID-19 causes an imbalance of bradykinins. The data show an improved prognosis with rising kallikrein levels, contradicting this notion. Kallistatin, which also increased over time among survivors in the study sample, balances out kallikrein, potentially balancing the rise in the kinin-kallikrein system. In addition to its pleiotropic effects on inflammation, endothelial function, and vascular repair, kallistatin has protective characteristics against acute lung injury. Kallistatin should be taken into consideration as a prospective applicant for clinical challenges in COVID-19, based on the data.

Even though prognostic analyses based on multiple measurements throughout time enable treatment tracking, including evaluating novel medications in clinical trials, prognostic evaluations from single time points are particularly helpful for the immediate handling of patients and resource allocation. So, to determine the outcome prognosis, the study applied an MLM to combine proteomic measures from the first-period opinion at WHO grade 7, i.e., invasive mechanical breathing and extra organ support therapy. Both in the exploratory cohort and in an entirely independent cohort (IC), this produces high prognostic values.

4.3 Transfer Learning

TL is a strategy that starts with a trained model for one task to solve other problems. As a result, pre-trained methods are utilized in TL as an alternative to time-consuming training using randomly initialised weights for specific tasks. The domain was explained as a tuple of pair elements made up of a feature space with a small chance of occurrence and a sample data point. The VGGNet16 model is utilised in this instance to record high-level semantic data.

4.3.1 VGGNet16

The VGGNet16 model is frequently utilised across a variety of areas due to its exceptional adaptability and relatively straightforward design. The ImageNet catalogue, which contains more than 14 million images and 1000 classes, shows that the VGGNet16 model has the highest testing accuracy at 92.7%. VGGNet16 is the name of the model since it has 16 layers. Thirteen convolution layers, ReLU, pooling, and three FC layers formation VGGNet16. Each max-pooling layer in the pre-trained VGGNet16's five blocks has a different level of specificity for the in-depth data. Local patterns are preserved by the lightweight layer whereas global patterns are obtained by the deep layer. The VGGNet16 design customs RGB pictures with a size of 224 224, a convolution network with a filter size of 3 3, and a pooling network with a filter size of 2 2, both with a pace of 1. The final component consists of three FC layers, each with 4096, 4096, and 1000 neurons.

The Softmax is the final layer, and it produces a statistical value of 0 or 1, which denotes the output class of the node. Every hidden layer has an AF that is provided by the ReLU layer.

$$K(x) = max(0, x) \quad (10)$$

When x is smaller than zero in equation (5), $K(x)$ is zero. $K(x) = x$ if x is better than or equivalent to zero. The VGGNet16 network does not employ local response normalisation (LRN), a normalisation technique that usages more resources and adds to the cost of computation while doing nothing to improve enactment on the ImageNet dataset. There are over 138 million trainable parameters in the VGGNet16 network. The aptitude of the organization approach will be enhanced and input data characterization learning will be

International Journal on Recent and Innovation Trends in Computing and Communication
ISSN: 2321-8169 Volume: 11 Issue: 9
***Article Received:** 25 July 2023 **Revised:** 12 September 2023 **Accepted:** 30 September 2023*

improved by fine-tuning the final layers. The specific tactic is to implement the GAP layer on the final block's PL. The GAP layer will be associated with first, then the FC1, and FC2 layers, and lastly, the output layer. The FC1, FC2, and yield layer weights are adjusted to gather domain-specific data, whereas the CL weights remain constant throughout model training.

5. Experimentation And Result Discussion

The data were processed with DIA-NN, an open-source programme for processing DIA / SWATH data (https://github.com/vdemichev/DiaNN, commit 4498bd7), using the previously described two-step spectral library refinement procedure with filtering at precursor level q-value (1%), library q-value (0.5%), and gene group q-value (1%). The study provides a COVID-19 CT image dataset, known as COVID-CT-MD (https://doi.org/10.6084/m9.figshare.13583015) that includes not individual COVID-19 patients nonetheless also healthy participants and those who have contracted community-acquired pneumonia (CAP). More specifically, COVID-CT-MD can help with the formation of cutting-edge ML and DNN-based systems.

Table 1. Simulation System Configuration

Simulation System Configuration	
MATLAB	Version R2020a
Operation System	Windows 10 Home
Memory Capacity	6GB DDR3
Processor	Intel Core i5 @ 3.5GHz
Simulation Time	10.190 seconds

The Matlab R2020a programme is employed to evaluate the recital of the suggested method. The program runs on the Windows 10 Home operating system and has a 6GB DDR3 memory capacity. The time required for simulation is 10.190 seconds using an Intel Core i5 @ 3.5GHz processor, as shown in table 1.

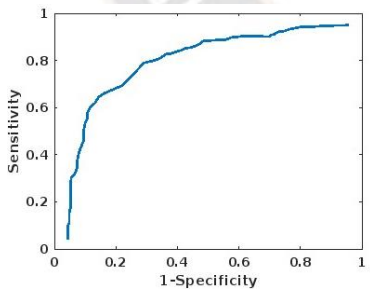

Figure 2. Forecast of D3 Nullification Level

Figure 2 shows the blood protein levels (Olink assay) predicted neutralisation levels at D3 (AUC 0.83, CI 0.80-0.85), with many proteins contributing to the prediction being independent of those linked with severity, however, this has to be confirmed in an self-governing dataset. Those complicated in the instruction of apoptosis (TNF superfamily members TNFSF10, galectin-7 [LG7BALS], and TNFSF8), phagocytosis (BRK1), T cell proliferation (IL-2), and tissue regeneration and proliferation (PTEN, EGFR, PLA2G10, RRM2, DKK3) were some of the proteins most frequently chosen in predicting neutralisation.

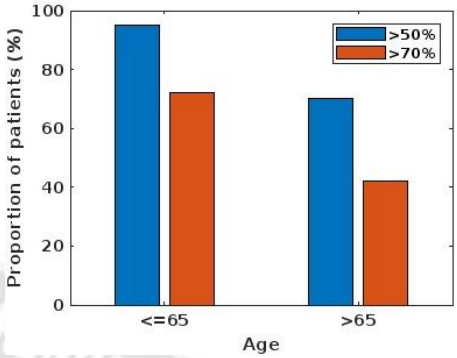

Figure 3. Proportion of Patients

Age-related comorbidities are shown in figure 3, as previously found, and show age-associated declines in both the rate of growth over time and the amount of neutralisation activity reached. The neutralisation activity was inversely correlated with age. Age had a detrimental effect on rapidly neutralisation increased with time, however only in patients who passed away (A1), suggesting that disease processes prevalent in severe illness also contribute to poor adaptive immune responses.

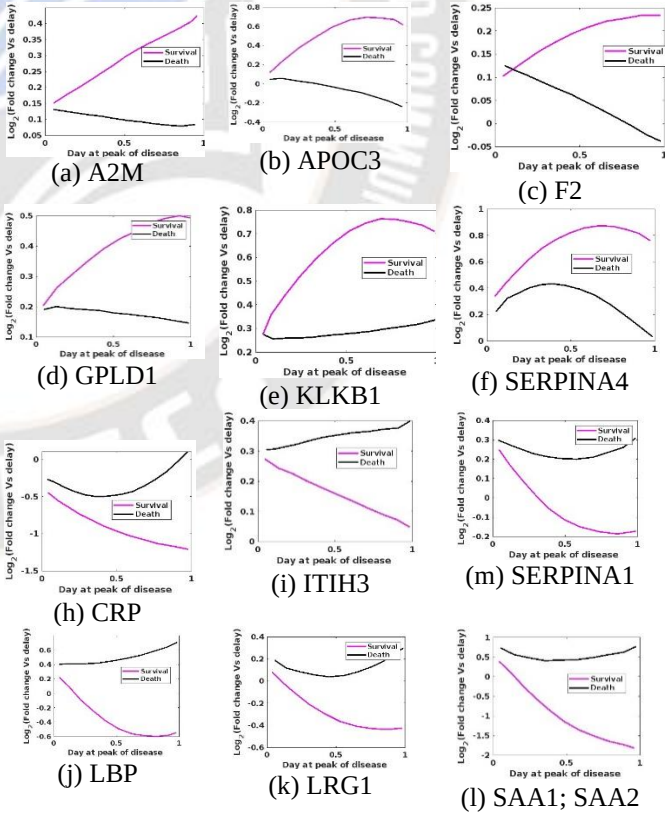

Figure 4. Protein Concentration Trajectories that Distinguish COVID-19 Survivors

International Journal on Recent and Innovation Trends in Computing and Communication
ISSN: 2321-8169 Volume: 11 Issue: 9
***Article Received:** 25 July 2023 **Revised:** 12 September 2023 **Accepted:** 30 September 2023*

Protein level trajectories across time (FDR 0.05) that distinguish between survivors and those who didn't survive in critically sick patients during the peak of the disease are represented by time-dependent concentration changes (y-axis: log2 fold change). Figure 4 shows that 12 of these proteins underwent distinct changes over time for survivors and non-survivors. A considerable rise in IP over time (SAA2, SAA1, ITIH3, CRP, LRG1, LBP, SERPINA10, and SERPINA1) was observed in patients with catastrophic outcomes. Additionally, in the plasma of survivors, these protein levels gradually dropped over time. Additionally, non-survivors levels of anti-IP (A2M, SERPINA4) declined with time, suggesting a persistent pro-IR. Similar to this, two crucial clotting system proteins, plasma kallikrein (KLKB1) and thrombin (F2), which are known to be diminished in severe COVID-19, continued to decline over time in non-survivors while increasing in survivors.

Series data is unfortunately impractical to gather for this purpose and the period for treatment decisions. So, we observed the possibility of predicting outcomes using single time point samples. To generate an outcome predictor, the study chose the latest example collected following the crucial choice regarding the growth treatment, i.e. the primary sample gained at the highest TL (WHO grade 7). The median number of days between sampling and outcome was 39 (IQR 16–64). Developed an MLM based on par enclitic networks, a graph-based approach in which networks representing the deviation of an individual from the population are derived, using 57 proteins for which targeted mass spectrometric assays (MRM assays) are listed in the MRM Assay DB, indicating that they have been selected for a clinical or biomedical indication also in another context. Every pair of analyses (proteins) is taken into account individually when producing the networks, and the EW is calculated as the predicted likelihood that a catastrophic event based on this pair of proteins would occur. To generate predictive models, it is then required to income into account the topological variations between networks from different scenarios (survivors vs. non-survivors) (Methods). By excluding the test individuals from the MLM's training, the study was able to predict outcomes with high accuracy.

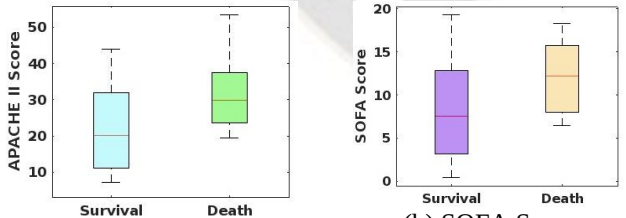

(a) APACHE II (b) SOFA Score

Figure 5. Prediction of Survival or Death in Critically Affected Patients

Presentation of recognised ICU risk assessment indices (APACHE II, Charlson comorbidity index, and SOFA mark) measured at the while of ICU admission (APACHE II, Charlson comorbidity index), or at the first-period opinion at WHO rating 7 (SOFA total) in predicting the forecast in disapprovingly sick patients. The Charlson Comorbidity Index fared poorly in separating survivors from non-survivors in this therapy group of severely sick COVID-19 patients, as shown in figure 5 with AUROC values of 0.63 (P = 0.16). Additionally, the APACHE II and SOFA marks were taken from a time-resolved data reserve for the PA-COVID-19 study, which contained a range of plasma proteomes, clinical parameters, enzyme activities, cell counts, and results. Both of these metrics, P = 0.05, AUROC = 0.68 for the APACHE II score at ICU charge and AUROC = 0.65, P = 0.11 for the SOFA groove at the stretch of the initial sample at WHO grade 7, were unable to meaningfully distinguish between survivors and non-survivors.

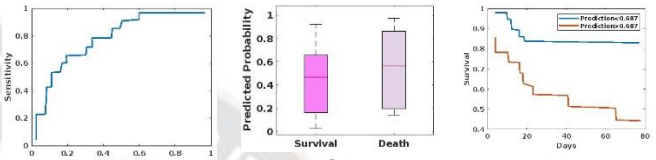

(a) (b) (c)

Figure 6. Prediction of Life Expectancy or Death in Critically Patients

The samples from the CC closest to the time point of therapy escalation during intensive care (start of ECMO, RRT, or vasopressors, i.e. WHO grade 7) were applied to build an MLM based on parenclitic networks (Methods). On the test samples, which were kept out during training, the enactment was evaluated. In the upper panel, the ROC curve demonstrates that survival vs. non-survival is correctly classified, with an AUROC of 0.81 (95% CI 0.68-0.94). The chance of endurance and non-survival was predicted using the proteomic classifier, and there is a substantial difference between the groups in the middle panel. Lower panel: Kaplan-Meier existence bends expending a predicted probability threshold of 0.678 that was selected to maximise the Youden J index (J = sensitivity + specificity—1). Patients with predictable demise risks of 0.678 (black) and > 0.678 (orange) were compared in terms of their survival rates using the log-rank test. Here, with AUC = 0.81 (95% CI 0.68-0.94) for the receiver-operating characteristic (ROC) curve in figure 6, obtained high prediction accuracy on the test subjects, who were excluded during training the MLM.

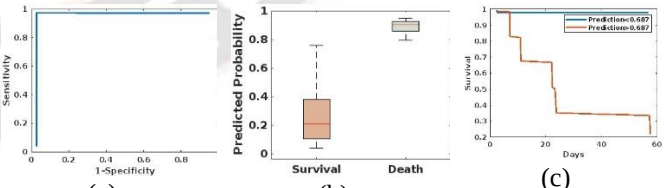

(a) (b) (c)

Figure 7. Model Trained on the Charite Cohort

Considered at the concert of the par enclitic system trained on the primary cohort (Charité) on an IC of 24 patients with critical COVID-19 from Austria (survival n = 19, death n = 5, median time among sampling and outcome 22 days, interquartile range 15-42 days) ('Innsbruck' cohort, Methods) to independently validate the potential of the plasma proteome to forecast outcomes in CI COVID-19 patients. Figure 7 shows

International Journal on Recent and Innovation Trends in Computing and Communication
ISSN: 2321-8169 Volume: 11 Issue: 9
***Article Received:** 25 July 2023 **Revised:** 12 September 2023 **Accepted:** 30 September 2023*

that the MLM has good predictive power on this IC despite the validation cohort coming from a different hospital and healthcare system (AUROC = 1.0, P = 0.000047). The algorithm accurately predicted the result for 18 out of 19 patients who endured and for 5 out of 5 patients who expired in this sovereign "Innsbruck" cohort using the cut-off value for existence forecast generated from the CC.

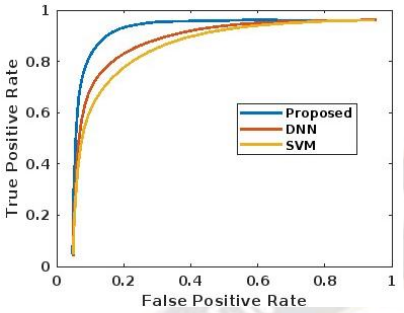

Figure 8. True Positive Rate Vs. False Positive Rate

Figure 8 portrays the comparison graph for the true optimistic rate and the false positive rate. It is compared with the existing DNN and SVM methods. Compared to these existing methods, the proposed method produces a higher value which is 0.96, and it produces more stable values than the other methods.

6. Research Conclusion

Globally, the COVID-19 disease of 2019 has been responsible for almost 1 million fatalities. Asymptomatic carriers to severe sickness, organ malfunction, and death are all possible outcomes of the disease1-4.5 Immune dysfunction, including both hyper- (activated inflammatory cascades, cytokine storm, tissue infiltrates, damage) and hypo-immune (relative lymphopenia, impaired T cell function, impaired interferon [IFN] antiviral responses, reduced viral permission) responses, is implicated in the pathophysiology of severe disease. In this work, a synonymic network is presented to accurately envisage the existence of CI patients in pre and post-COVID-19. Initially, the GLCM is proposed to extract features from the IRs. It confirms the COVID-19-IR s. This work implemented a variety of features using CT images with a CNN-based Inception V3 model for selection algorithms to filter significant features. The VGGNet16 model is subsequently shown, which has the probability to gather high-level semantic data and further categorise the severity of the condition. Utilising the Matlab programme, the suggested task is assessed. The training times of different deep learning procedures are in this order, according to the results, with VGGNet-16 (402 s) taking the longest. The study evaluated the routine of the synolytic network trained on the prime cohort on an IC of CI COVID-19 patients from the database, to independently assess the capability of the plasma and serum proteome to envisage consequences in COVID-19 patients. Extensive experiments were implemented and the results demonstrated the advantage of the proposed methods. The range below the receiver operating characteristic (ROC) curve (AUC) was 83%, the zone under the precision-recall curve (PRAUC) was 95%, and accuracy, sensitivity 96.7%, and specificity 98.2% were calculated to quantify the prediction enactment of the model. The suggested approach outperforms other existing methods, such as DNN and SVM, in terms of routine and accurately expects existence in disapprovingly sick patients in pre- and post-COVID-19 from single blood samples, weeks earlier than the outcome.

References

[1] E.S. Goudouris, "Laboratory diagnosis of COVID-19," Jornal de pediatria, vol. 97, pp.7-12, 2021.
[2] A.P. Beltrami, M. De Martino, E. Dalla, M.C. Malfatti, F. Caponnetto, M. Codrich, D. Stefanizzi, M. Fabris, E. Sozio, F. D'Aurizio, and C.E. Pucillo, "Combining Deep Phenotyping of Serum Proteomics and Clinical Data via Machine Learning for COVID-19 Biomarker Discovery," International Journal of Molecular Sciences, vol. 23, no. 16, pp.9161, 2022.
[3] V. Demichev, P. Tober-Lau, T. Nazarenko, O. Lemke, S. Kaur Aulakh, H.J. Whitwell, A. Röhl, A. Freiwald, M. Mittermaier, L. Szyrwiel, and D. Ludwig, "A proteomic survival predictor for COVID-19 patients in intensive care," PLOS Digital Health, vol. 1, no. 1, pp. e0000007, 2022.
[4] S.A. Vajiha Begum, M. Pushpa Rani, "Recognition of neurodegenerative diseases with gait patterns using double feature extraction methods," IEEE - 2020 4th International Conference on Intelligent Computing and Control Systems (ICICCS), pp. 332-338, 2020, 10.1109/ICICCS48265.2020.9120920
[5] A.D. Whetton, G.W. Preston, S. Abubeker, and N. Geifman, "Proteomics and informatics for understanding phases and identifying biomarkers in COVID-19 disease," Journal of proteome research, vol. *19*, no. 11, pp.4219-4232, 2020.
[6] R. Rana, V. Rathi, and N.K. Ganguly, "A comprehensive overview of proteomics approach for COVID-19: new perspectives in target therapy strategies," Journal of Proteins and Proteomics, vol. 11, no. 4, pp.223-232, 2020.
[7] V.R. Richard, C. Gaither, R. Popp, D. Chaplygina, A. Brzhozovskiy, A. Kononikhin, Y. Mohammed, R.P. Zahedi, E.N. Nikolaev, and C.H. Borchers, "Early prediction of COVID-19 patient survival by targeted plasma multi-omics and machine learning," Molecular & Cellular Proteomics, vol. 21, no. 10, 2022.
[8] A. McArdle, K.E. Washington, B. Chazarin Orgel, A. Binek, D.M. Manalo, A. Rivas, M. Ayres, R. Pandey, C. Phebus, K. Raedschelders, and J. Fert-Bober, "Discovery proteomics for COVID-19: where we are now," Journal of Proteome Research, vol. 20, no. 10, pp.4627-4639, 2021.
[9] Athi sakthi, Pushpa Rani, "Detection of Movement Disorders Using Multi SVM," Global Journal of Computer Science and Technology, vol. 13, no.1, pp. 23-25, 2013.
[10] P. Manickam, S.A. Mariappan, S.M. Murugesan, S. Hansda, A. Kaushik, R. Shinde, and S.P. Thipperudraswamy, "Artificial intelligence (AI) and the internet of medical things (IoMT) assisted biomedical systems for intelligent healthcare," Biosensors, vol. 12, no. 8, pp.562, 2022.
[11] M.A. Al-Nesf, H.B. Abdesselem, I. Bensmail, S. Ibrahim, W.A. Saeed, S.S. Mohammed, A. Razok, H. Alhussain, R. Aly, M. Al Maslamani, and K. Ouararhni, "Prognostic tools and candidate drugs based on plasma proteomics of patients with severe COVID-19 complications," Nature communications, vol. 13, no. 1, pp.1-14, 2022.
[12] H. Singh, R. Nema, and A. Kumar, "Genomic, proteomic biomarkers and risk factors associated with COVID-19," In Advanced Biosensors for Virus Detection, pp. 95-111, Academic Press, 2022.
[13] M. Buyukozkan, S. Alvarez-Mulett, A.C. Racanelli, F. Schmidt, R. Batra, K.L. Hoffman, H. Sarwath, R. Engelke, L. Gomez-Escobar, W. Simmons, and E. Benedetti, "Integrative Metabolomic and Proteomic Signatures Define Clinical Outcomes in Severe COVID-19," medRxiv, pp.2021-07, 2022.

[14] A. Komathi, M. Pushpa Rani, "Trust performance of AODV, DSR and DSDV in wireless sensor networks," IEEE - Second International Conference on Current Trends In Engineering and Technology," pp. 423-425, 2014.
[15] M. Davis, and B.I. Morshed, "Classification of COVID-19 Disease Severity using CT Scans via Deep Convolutional Neural Networks," In 2022 IEEE International Conference on Electro Information Technology (eIT), pp. 401-404, 2022, May, IEEE.
[16] A.K. Tyagi, and P. Chahal, "Artificial intelligence and machine learning algorithms," In Research Anthology on Machine Learning Techniques, Methods, and Applications, pp. 421-446, 2022. IGI Global.
[17] R. Sardar, A. Sharma, and D. Gupta, "Machine learning assisted prediction of prognostic biomarkers associated with COVID-19, using clinical and proteomics data," Frontiers in genetics, pp.522, 2021.
[18] A. Kruger, M. Vlok, S. Turner, C. Venter, G.J. Laubscher, D.B. Kell, and E. Pretorius, "Proteomics of fibrin amyloid micro clots in long COVID/post-acute sequelae of COVID-19 (PASC) shows many entrapped pro-inflammatory molecules that may also contribute to a failed fibrinolytic system," Cardiovascular Diabetology, vol. 21, no. 1, pp.1-23, 2022.
[19] G.G. Chiddarwar, S.V. Balshetwar, B.P. Vasgi, "Blockchain based record date management system using artificial intelligence," Neuroquantology, vol. 20, no. 11, pp. 3847-3853, 2022.
[20] W. Chen, M. Yao, Z. Zhu, Y. Sun, and X. Han, "The application research of AI image recognition and processing technology in the early diagnosis of COVID-19," BMC Medical Imaging, vol. 22, no. 1, pp.1-10, 2022.
[21] A. Komathi, M. Pushpa Rani, "Shift reduce parser based malicious sensor detection for predicting forest fire in WSNs," Wireless Personal Communications, vol. 103, pp. 2843-2861, 2018.
[22] H. Yan, X. Liang, J. Z. Du, He, Y. Wang, M. Lyu, L. Yue, F. Zhang, Z. Xue, L. Xu, and G. Ruan, "Proteomic and Metabolomic Investigation of COVID-19 Patients with Elevated Serum Lactate Dehydrogenase," medRxiv, 2021.
[23] PA-COVID-19 Study group, "A proteomic survival predictor for COVID-19 patients in intensive care," PLOS Digital Health, 2022.
[24] M.R. Trugilho, I.G. Azevedo-Quintanilha, J.S. Gesto, E.C.S., Moraes, S.C., Mandacaru, M.M., Campos, D.M., Oliveira, S.S. Dias, V.A. Bastos, M.D. Santos, and P.C. Carvalho, "Platelet proteome reveals features of cell death, antiviral response and viral replication in covid-19," Cell Death Discovery, vol. 8, no. 1, pp.1-11, 2022.
[25] Z. Zhang, F. Lin, F. Liu, Q. Li, Y. Li, Z. Zhu, H. Guo, L. Liu, X. Liu, W. Liu, and Y. Fang, "Proteomic profiling reveals a distinctive molecular signature for critically ill COVID-19 patients compared with asthma and chronic obstructive pulmonary disease," International Journal of Infectious Diseases, vol. 116, pp.258-267, 2022.
[26] B.T. Steffen, J.S. Pankow, P.L. Lutsey, R.T. Demmer, J.R. Misialek, W. Guan, L.T. Cowan, J. Coresh, F.L. Norby, and W. Tang, "Proteomic profiling identifies novel proteins for genetic risk of severe COVID-19: the Atherosclerosis Risk in Communities Study," Human Molecular Genetics, 2022.
[27] R.C. Poulos, Z. Cai, P.J. Robinson, R.R. Reddel, and Q. Zhong, "Opportunities for pharmacoproteomics in biomarker discovery. Proteomics, pp.2200031, 2022.
[28] S.S. Foo, M.C. Cambou, T. Mok, V.M. Fajardo, J K.L. ung, T. Fuller, W. Chen, T. Kerin, J. Mei, D. Bhattacharya, and Y. Choi, "The systemic inflammatory landscape of COVID-19 in pregnancy: Extensive serum proteomic profiling of mother-infant dyads with in utero SARS-CoV-2," Cell Reports Medicine, vol. 2, no. 11, pp.100453, 2021.
[29] S. Yasar, Z. Kucukakcali, and A. Doganer, "Ensemble learning-based prediction of COVID-19 positive patient groups determined by IL-6 levels and control individuals based on the proteomics data," Medicine, vol. 10, no. 4, pp.1516-23, 2021.
[30] D.R.S. Junior, A.R.M. Silva, L. Rosa-Fernandes, L.R. Reis, G. Alexandria, S.D. Bhosale, F. de Rose Ghilardi, T.F. Dalçóquio, A.J. Bertolin, J.C. Nicolau, and C.R. Marinho, "HDL proteome remodelling is associates with COVID-19 severity," Journal of clinical lipidology, vol. 15, no. 6, pp.796-804, 2021.
[31] Nihar Ranjan Kar, "Advancement Of Artificial Intelligence In Pharmacy: A Review," Shodhsamhita, vol. IX, no. (II(IV)), pp. 514-529, 2022.
[32] Nihar Ranjan Kar, "Osmotically Controlled Drug Delivery Systems: A Review," Indian Journal of Natural Sciences, vol. 13, no. 72, pp. 43372-43394, 2022.
[33] Nihar Ranjan Kar, "Nanotechnology-Based Targeted Drug Delivery Systems for Brain Tumors," Indian Journal of Natural Sciences, vol. 12, no. 68, 35081-35094, 2021.
[34] Nihar Ranjan Kar, "Liposomal Drug Delivery System: An Overview," Shodhasamhita: Journal of Fundamental & Comparative Research, vol. VIII, no. 5, pp. 123-134, 2022.
[35] Nihar Ranjan Kar, "A Review on Targeting of Drugs to Brain," Indian Journal of Natural Sciences, vol. 11, no. 64, pp. 2021.
[36] Nihar Ranjan Kar, "Niosomal Drug Delivery System: An Overview," Madhya Bharti, vol. 82, no. 14, pp. 180-190, 2022.
[37] Nihar Ranjan Kar, "Nutraceuticals in Pharmaceutical Field," Indian Journal of Natural Sciences, vol. 13, no. 72, pp. 43165-43171, 2022.
[38] Nihar Ranjan Kar, "Subas Chandra Dinda. Colon Specific Drug Delivery System: An Approach to Target Colonic Diseases," International Journal of Pharmaceutical Sciences and Research, vol. 10, no. 3, pp.1080-1088, 2019;
[39] Nihar Ranjan Kar, Subas Chandra Dinda, "Formulation and in vitro Characterization of Metronidazole Loaded Polymeric Microspheres for Colon Specific and Sustained Drug Delivery," Pharm Methods, vol. 10, no. 1, pp. 1-8, 2019;
[40] A.P. Senthil Kumar, S. Yuvaraj, S. Janaki, "Experimental investigations of Co3O4, SiO2, cotton seed oil additive blends in the diesel engine and optimization by ANN-SVM process," Journal of Ceramic Processing Research, vol. 21, no. 2, pp. 217-225, 2020.
[41] S. Yuvaraj, A.P. Senthil Kumar, M. Muthukumar, K. Sadesh, S. Janaki, "Certain studies on influence of nano catalysts Co3O4, SiO2 blended with CME-diesel in combustion," Materials Today: Proceedings, vol. 51, pp. 1612-1618, 2022.
[42] B.C. Anil & P. Dayananda, "Automatic Liver Tumor Segmentation based on Multi-level Deep Convolutional Networks and Fractal Residual Network," IETE Journal of Research, vol. 69, no. 4, pp. 1925-1933, 2023, DOI: 10.1080/03772063.2021.1878066
[43] B. C. Anil, P. Dayananda, B. Nethravathi & M. S. Raisinghani, "Efficient Local Cloud-Based Solution for Liver Cancer Detection Using Deep Learning," International Journal of Cloud Applications and Computing (IJCAC), vol. 12, no. 1, pp. 1-13, 2022, http://doi.org/10.4018/IJCAC.2022010109
[44] B. Nethravathi & S. Sinchana & C. Anil, "Advanced Face Recognition Based Door Unlock System using Arduino," International Journal of Recent Technology and Engineering (IJRTE), vol. 8, pp. 7844-7848, 2020, 10.35940/ijrte.C6541.098319.
[45] B.C. Anil, & P. Dayananda, "Study on Segmentation and Liver Tumor Detection Methods," International Journal of Engineering and Technology(UAE), vol. 7, pp. 28-33, 2018, 10.14419/ijet.v7i3.4.14670.
[46] Shyam Sunder Bahety, Kishan Kumar, Vishwadeep Tejaswi, R. Sharad Balagar, B.C. Anil, "Implementation of Automated Attendance System using Facial Identification from Deep Learning Convolutional Neural Networks," INTERNATIONAL JOURNAL OF ENGINEERING RESEARCH & TECHNOLOGY (IJERT) NCAIT – 2020, vol. 8, no. 15, 2020.
[47] R.K. Pattanaik, S. Mishra, M. Siddique, T. Gopikrishna, S. Satapathy, "Breast Cancer Classification from Mammogram Images Using Extreme Learning Machine-Based

DenseNet121 Model," Genetics Research, pp. 2731364, 2022.
[48] S.K. Mohapatra, S. Prasad, G.M. Habtemariam, M. Siddique, "Identify determinants of infant and child mortality based using machine learning: Case study on Ethiopia," Big Data Analytics and Machine Intelligence in Biomedical and Health Informatics: Concepts, Methodologies, Tools and Applications, pp. 21–45, 2022.
[49] M. Siddique, D. Panda, "Prediction of stock index of tata steel using hybrid machine learning based optimization techniques," International Journal of Recent Technology and Engineering, vol. 8, no. 2, pp. 3186–3193, 2019.
[50] M. Siddique, D. Panda, "A hybrid forecasting model for prediction of stock index of tata motors using principal component analysis, support vector regression and particle swarm optimization," International Journal of Engineering and Advanced Technology, vol. 9, no. 1, pp. 3032–3037, 2019.
[51] Tarun Kumar Kotteda, Manoj Kumar, Pramod Kumar, Rama Bhadri Raju Chekuri, "Metal matrix nanocomposites: future scope in the fabrication and machining techniques," The International Journal of Advanced Manufacturing Technology, 2022. https://doi.org/10.1007/s00170-022-09847-0
[52] Tarun Kumar Kotteda, Rama Bhadri Raju Chekuri, Naga Raju, Prasada Raju Kantheti, S. Balakumar, "Analysis on Emissions and Performance of Ceramic Coated Diesel Engine Fueled with Novel Blends Using Artificial Intelligence," Advances in Materials Science and Engineering, 2021, https://doi.org/10.1155/2021/7954488
[53] S. S. Reddy, N. Sethi, R. Rajender, & V.S.R. Vetukuri, "Non-invasive diagnosis of diabetes using chaotic features and genetic learning," In Third International Conference on Image Processing and Capsule Networks, pp. 161–170, 2022. Cham: Springer International Publishing.
[54] S. S. Reddy, L. Alluri, M. Gadiraju, & R. Devareddi, "Forecasting Diabetic Foot Ulcers Using Deep Learning Models," Proceedings of Third International Conference on Sustainable Expert Systems, pp 211–227, 2023.
[55] R. S. Shankar, D. R. Babu, K.V.S.S. Murthy, & V. Gupta, 'An approach for essay evaluation using system tools," 2017 International Conference on Innovative Research In Electrical Sciences (IICIRES). IEEE. 2017.
[56] R. Shiva Shankar, & D. Ravibabu, "Digital report grading using NLP feature selection," In Soft Computing in Data Analytics,615–623, 2019. Proceedings of International Conference on SCDA 2018.
[57] Reddy, Shiva Shankar, M. Gadiraju, & V.V.R. Maheswara Rao, "Analyzing student reviews on teacher performance using long short-term memory," In Innovative Data Communication Technologies and Application, pp. 539–553, 2022. Singapore: Springer Nature Singapore.
[58] N. Mary Peter, M. Pushpa Rani, "V2V communication and authentication: the internet of things vehicles (IoTV)," Wireless Personal Communications, vol.120, no.1, pp. 231-247, 2021.